Influences of turbulence on suspension feeding by planktonic protozoa; experiments in laminar shear fields

Jeff Shimeta,[1] Peter A. Jumars, and Evelyn J. Lessard
School of Oceanography, Box 357940, University of Washington, Seattle 98195-7940

Abstract

Laminar shear below the turbulence microscale can create relative motion between protozoan suspension feeders and their prey, potentially influencing encounter and retention. Theory suggests that ingestion rate may rise sigmoidally with increasing turbulence strength, although interference with feeding mechanisms might occur at some turbulence levels. We measured rates of feeding on fluorescently labeled prey at concentrations below feeding saturation in a survey of cultured bacterivorous and herbivorous flagellates, ciliates, and a helioflagellate over a wide range of shear rates produced in rotating Couette flows. Shears of 0.1–10 s^{-1} (corresponding to moderate to extremely strong marine and estuarine turbulence) enhanced clearance rates by the aloricate choanoflagellate, *Monosiga* sp., up to 2.7× the mean rate in still water. Shears of 1–10 s^{-1} enhanced clearance rates by the helioflagellate, *Ciliophrys marina,* up to 7.0× the mean in still water. The data are consistent with a sigmoidal response to increasing shear rate. In contrast, clearance rates of the tintinnid, *Helicostomella* sp., were suppressed at 10 s^{-1} to as low as 0.42× the still-water rate. Several other flagellates and ciliates (*Paraphysomonas* sp., two unidentified chrysomonads, *Diaphanoeca grandis, Favella* sp., and an unidentified heterotrich) showed no significant effects. We hypothesize that the protozoa most susceptible to an influence of turbulence are nonmotile (e.g. Heliozoa, Foraminifera, Radiolaria) or are weak swimmers (e.g. some flagellates and ciliates). Current methods for measuring feeding rates in still-water incubations may underestimate grazing by these taxa under strong turbulence in the field. Through species-specific influences on feeding rates, spatial and temporal variations in turbulence may have very selective effects on microbial food-web dynamics.

Protozoan suspension feeders are important grazers of bacteria and phytoplankton in planktonic, microbial food webs. Their feeding depends on a flux of prey cells to their capturing structures, which traditionally has been believed to be controlled by a feeding current and (or) prey motion (Fenchel 1987), as well as on the ability to retain and manipulate encountered cells. Influences of ambient fluid motion on particle encounter and retention, however, have rarely been addressed. Such effects would create a coupling between dynamics of the physical environment and feeding rates (presumably also growth rates) in microbial food webs.

At length scales smaller than the lower limit, or microscale, of turbulence, viscosity smoothes out turbulent velocity fluctuations into a laminar shear field (Lazier and Mann 1989). Protozoan suspension feeders generally are smaller than the turbulence microscale in the surface mixed layer (order 1–10 mm), and the laminar shear they experience may produce relative motion between them and their food particles. Studies of feeding mechanisms and rates, however, are typically made under conditions of little or no fluid motion (Fenchel 1980, 1982a; Sherr et al. 1989). A few experiments and anecdotal observations suggest that agitation influences protozoan growth in cultures (Berdalet 1992; Hellung-Larsen and Lyhne 1992). It has not been known whether rates of particle encounter or feeding are influenced by the shear experienced in environmental turbulence.

Notation

A	Hamaker constant, J
C	Particle concentration, m^{-3}
CR	Clearance rate, ml h^{-1}
D	Prey diffusivity, m^2 s^{-1}
E_C, E_t	Collision efficiency in Couette flow and in turbulence, dimensionless
F_1	Encounter rate, s^{-1}
G_C	Mean shear rate in Couette flow, s^{-1}
G_t	Mean laminar shear rate below the turbulence microscale, s^{-1}
Pe_F, Pe_S	Peclet number as a ratio of either advection or shear to diffusion, nondimensional
p	Radius ratio, r_2/r_1, dimensionless
R_1, R_2	Inner and outer radius of gap in Couette tank, m
r_1, r_2	Radius of protozoan cell and food particle, or radii of spheres, m
U	Swimming speed, m s^{-1}
ε	Mean turbulent kinetic energy dissipation rate per unit of mass, W kg^{-1}
ε_{cons}	Conservative estimate of ε (Eq. 9), W kg^{-1}
ε_{cr}, $\varepsilon_{(cons)cr}$	Critical values of ε and ε_{cons} for turbulence to influence encounter rate, W kg^{-1}
η	Kolmogorov length microscale of turbulence, m
θ	Bottom angle in Couette tank, rad
ν	Kinematic viscosity of seawater, 1×10^{-6} m^2 s^{-1}
ω	Rotation rate of Couette tank, rad s^{-1}

Theory

The Kolmogorov length microscale of turbulence is

$$\eta = \left(\frac{\nu^3}{\varepsilon}\right)^{1/4} \qquad (1)$$

[Tennekes and Lumley 1972; often used operationally as $\eta = 2\pi(\nu^3/\varepsilon)^{1/4}$, Lazier and Mann 1989] where ε is the mean rate of dissipation of turbulent kinetic energy per unit of mass and ν is kinematic viscosity. (A list of notation is provided.) Values of ε in the ocean typically are in the range 10^{-10}–10^{-3} W kg^{-1} (Yamazaki and Osborn 1988), with high values in surface-mixed layers of the open ocean being 10^{-5} W kg^{-1} (Gargett 1989) and in the coastal ocean up to 10^{-2} W kg^{-1} in tidal channels (Wesson and Gregg 1994). In isotropic turbulence, the mean shear rate below η can be expressed as

$$G_t = 0.365 \left(\frac{\varepsilon}{\nu}\right)^{1/2} \qquad (2)$$

(Lazier and Mann 1989), although coefficients ranging from 0.18 to 1.0 have been used in place of 0.365 in this expression (Batchelor 1980; Thomas and Gibson 1990; Bowen et al. 1993). For strong turbulence of 10^{-6}–10^{-5} W kg^{-1}, η is therefore of order 1 mm and G_t is of order 1 s^{-1}.

In isotropic turbulence, shear-driven contact rates by direct interception between submicroscale spheres were modeled by Saffman and Turner (1956) as

$$F_1 = 1.3 (r_1 + r_2)^3 \left(\frac{\varepsilon}{\nu}\right)^{1/2} E_t C_2. \qquad (3)$$

F_1 is the rate of encounter between a single sphere of radius r_1 and spheres of radius r_2, E_t is the collision efficiency in submicroscale shear, and C_2 is the concentration of sphere 2. $E_t \approx 1$ for p ($=r_2/r_1$) ≈ 0.5–1 (Saffman and Turner 1956), and $E_t \approx 7.5$ $[p^2/(1+2p)^2]$ for $p \ll 1$ (Hill 1992). Shimeta and Jumars (1991) applied Eq. 3 with $\varepsilon = 10^{-6}$–10^{-5} W kg^{-1} and $E_t = 1$ to calculate encounter rates for specific protozoa and food particles and compared them with published feeding rates in still water. The ratio of F_1 to measured feeding rate ranged from order 10^{-2} to order 1 for both flagellates and ciliates, and we suggested that in some cases ambient shear has the potential to influence feeding rates.

Turbulence strength must exceed some critical level, however, before the encounter rate effected by submicroscale shear exceeds that caused by other mechanisms (Fig. 1), namely feeding currents and prey motion (Brownian or behavioral). Below this threshold, ε_{cr}, encounter rate should be independent of dissipation rate (Fig. 1, region A); above ε_{cr}, encounter rate should rise monotonically (regions B and C). Through regions A and B, ingestion rate follows the encounter-rate curve in shape if the efficiencies of retention and ingestion are constant and also in magnitude if all encountered particles are consumed. At high encounter rates, a processing-rate limitation must occur (region C), resulting in feeding-rate saturation and thus an ingestion curve resembling a sigmoidal or Type 3 functional response (Real 1977). (Note that the ingestion-rate curve would remain sigmoidal if plotted against shear rate.)

The existence, shape, and extent of each region of the curves in Fig. 1 are likely to vary among species and feeding circumstances. Encounter-rate curves in regions B and C may differ in shapes and magnitudes from Eq.
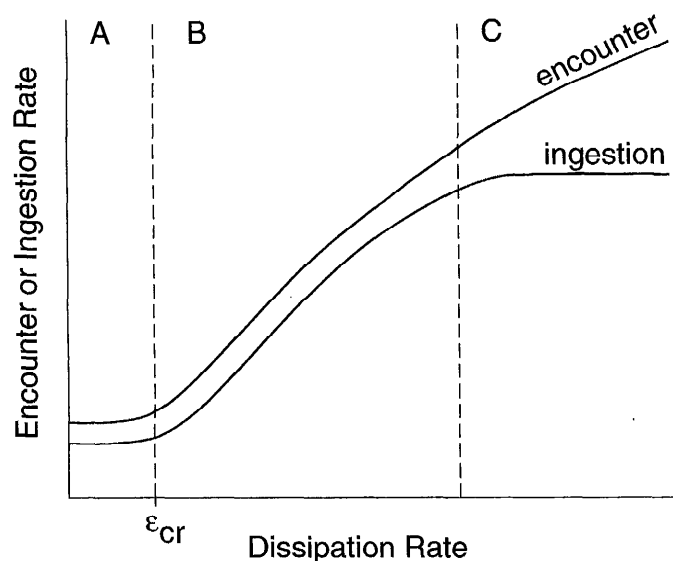
Fig. 1. Qualitative prediction of encounter rate and ingestion rate as functions of turbulent dissipation rate. ε_{cr} = critical dissipation rate required for shear-driven particle flux to exceed that due to a feeding current or prey motion. It is assumed for demonstration that not all encountered particles are retained for ingestion. Refer to text for discussion of regions A, B, and C.

3 because of the various morphologies and feeding mechanisms of protozoa (requiring modification of F_t). Region B would not exist for the ingestion-rate curve if high food concentrations cause feeding-rate saturation at all levels of turbulence. If ε_{cr} is large, region B may exist only at uncommonly high dissipation rates and be irrelevant under most field conditions. An additional possibility not shown is that ambient shear interferes with particle encounter and (or) handling, resulting in a negative slope somewhere in either curve.

Rough estimates of ε_{cr} can be hypothesized by using scaling parameters in analogy to mass transfer to submicroscale spheres in turbulence. We caution that the strict applicability of these models to protozoa is suspect without accounting for morphologies and feeding mechanisms. For a given protozoan and prey cell, one can first estimate whether feeding-current advection or prey motion (the latter modeled as diffusion) predominates in turbulence weaker than ε_{cr} by calculating a feeding-current Peclet number ($\mathrm{Pe}_F = r_1 U/D$, where r_1 is protozoan radius,

U is protozoan swimming or feeding-current speed, and D is prey diffusivity). For $\mathrm{Pe}_F \gg 1$ (advection predominates), one can then estimate ε_{cr} by incorporating Batchelor's (1980) result for the balance between shear and advection in driving mass transfer from a translating sphere:

$$\varepsilon_{cr} = 0.6\left(\frac{U}{r_1}\right)^2 \nu; \quad \mathrm{Pe}_F \gg 1. \tag{4}$$

Calculations with Eq. 4 suggest that shear can dominate particle flux to the slowest flagellates and ciliates (i.e. those with the weakest feeding currents) under very strong turbulence (Table 1). For $\mathrm{Pe}_F \ll 1$, one can estimate ε_{cr} with a shear-Pe (Pe_S) representing the balance of ambient shear and prey diffusion. Substituting Eq. 2 into $\mathrm{Pe}_S = r_1^2 G_t/D$ and setting $\mathrm{Pe}_S = 1$ yields

$$\varepsilon_{cr} = 7.5\left(\frac{D}{r_1^2}\right)^2 \nu; \quad \mathrm{Pe}_F \ll 1. \tag{5}$$

Calculations with Eq. 5 suggest that weak turbulence might influence encounter of nonmotile protozoa (i.e. sarcodines: Heliozoa, Foraminifera, Radiolaria) with bacteria or nonmotile algae, while strong turbulence might influence their encounter with flagellates (Table 2).

We measured feeding rates of nine protozoan species using nonmotile (heat-killed) bacteria and algae under imposed, steady, laminar shear (Couette flows). Particle dynamics (at least of spheres) in simple shear flow can differ from those in 3-dimensional shear (*see discussion*), so our quantitative results cannot be considered explicit tests of Eq. 3–5 applied to protozoa in natural turbulence. Nonetheless, a comparison of our results with a model of encounter in Couette flow suggests that these protozoan cells do not behave like spheres in simple shear and furthermore that any artifact of Couette flow is likely to produce underestimates of the influence of environmental turbulence on feeding.

Materials and methods

Couette tanks—Three identical Couette tanks were used (Fig. 2). The outer cylindrical acrylic cup is bolted to the rotating platter. The removable inner PVC cylinder is centered by the spindles and tank cover and is kept from rotating by a catch rod attached above. As the outer cyl-

Table 1. Estimates of ε_{cr} calculated by analogy to mass transfer to spheres, using Eq. 4.

Protozoan cell	r_1 (μm)	U (μm s^{-1})*	Food particle	ε_{cr} (W kg^{-1})
Flagellate	2.5	20–200†	Nonmotile or motile bacterium	4×10^{-5}–4×10^{-3}
Ciliate	50	200–1,000	Any cell	1×10^{-5}–2×10^{-4}

* Values from Roberts (1981), Fenchel (1987), and Buskey et al. (1993).
† U must be $>40\ \mu$m s^{-1} to satisfy $\mathrm{Pe}_F > 1$ when considering a motile bacterium ($D = 1\times10^{-6}$ cm^2 s^{-1}; Fenchel 1982*a*).

Table 2. Estimates of ε_{cr} calculated by analogy to mass transfer to spheres, using Eq. 5.

Protozoan cell	r_1 (μm)	Food particle	D (cm^2 s^{-1})	ε_{cr} (W kg^{-1})
Flagellate*	2.5	Motile bacterium	1×10^{-6}†	2×10^{-3}
Sarcodine	50	Nonmotile bacterium	4×10^{-9}‡	2×10^{-13}
		Motile bacterium	1×10^{-6}†	1×10^{-8}
		Nonmotile alga	4×10^{-10}‡	2×10^{-15}
		Flagellate	1×10^{-5}–1×10^{-4}§	1×10^{-6}–1×10^{-4}
		Ciliate	1×10^{-2}‖	1×10^{0}

* U must be <40 μm s^{-1} to satisfy Pe$_F$ < 1 when considering a motile bacterium.
† Fenchel 1982a.
‡ Calculated Brownian diffusivity (Shimeta and Jumars 1991); nonmotile alga with $r_2 = 5$ μm.
§ Calculated by assuming step length is similar to that of ciliates (Jonsson 1989).
‖ Jonsson 1989.

inder turns, the fluid in the gap is sheared. The platter is mounted on a support and turned by a variable-speed D.C. motor controlled by a digital voltage switch. Motors of differing gear ratios were interchanged among the tanks to produce different ranges of shear-rate settings. The mean shear rate across the side gap is

$$G_{\mathrm{C}} = \frac{2\omega R_1 R_2}{R_2^2 - R_1^2}. \tag{6}$$

R_1 and R_2 are the inner and outer radius of the gap, respectively, and ω is the rotation rate in radians per unit

of time (van Duuren 1968). The mean shear rate across the bottom, wedge-shaped gap is

$$G_{\mathrm{C}} = \frac{\omega}{\theta} \tag{7}$$

where θ is the bottom angle in radians (Van Wazer et al. 1963). In all three tanks, $R_1 = 5.4$ cm, $R_2 = 5.7$ cm, and $\theta = 0.054$ rad. The angle was chosen such that G_{C} is equivalent in the side and bottom, minimizing the end effect. For these dimensions, the shear rate is approximately constant (i.e. linear shear). A slight curvature of the shear occurs near the walls, but the shear rate at the side wall deviates by $\leq 6\%$ from the mean (calculated according to van Duuren 1968). In the bottom gap, shear rate is independent of radial position, and for $\theta \lesssim 0.053$ rad, the shear rate is approximately constant across the gap (Van Wazer et al. 1963). The flow within the tanks was strictly laminar. The critical ω for transition to turbulent flow is 12 rad s^{-1} (calculated according to van Duuren 1968) but ω never exceeded 1.3 rad s^{-1} in experiments.

Organisms and stock cultures—Cultures (Table 3) were kept in 100-ml volumes in acid-washed 250-ml polycarbonate flasks, stored under dim light, and transferred monthly to fresh media. Media were based on GF/F-filtered, heat-sterilized Puget Sound seawater (~ 27‰). "Ciliate medium" contained added trace metals and vitamins (f medium mixtures at f/200 and f/10 levels, respectively; Guillard 1975) and 10^{-7} M Na$_2$-EDTA. Media for bacterivores contained 0.01% yeast extract to support a resident mixed assemblage of marine bacteria. Herbivores were fed weekly with phytoplankton, which were cultured in f/2-Si medium (Guillard 1975).

Preparation of FLB and FLA—Fluorescently labeled bacteria (FLB) and algae (FLA) were heat killed and stained with DTAF following the method of Sherr and Sherr (1993), with Na$_4$P$_2$O$_7$ buffers reduced to 0.002 M. Fluorescently labeled *Escherichia coli* minicells (FLm), ~ 0.6 μm, were used in experiments with all bacterivores except *Ciliophrys*. *E. coli* strain χ-1488 was obtained from the
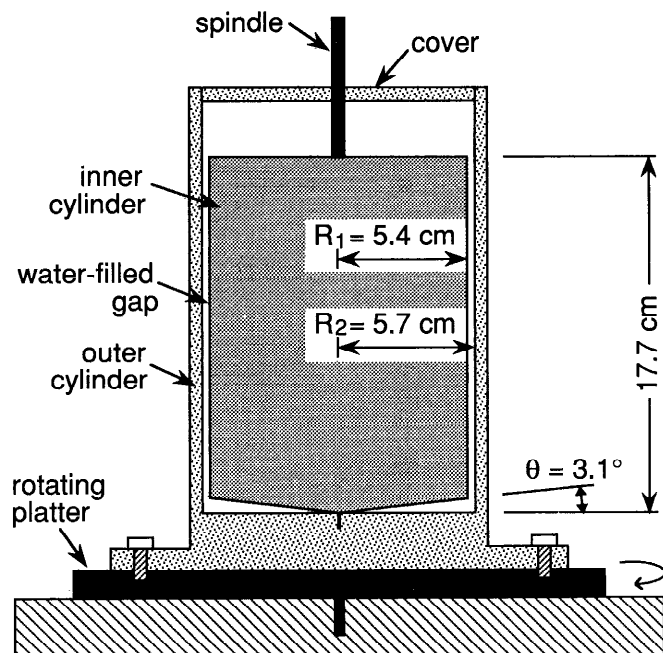

Fig. 2. Design of the Couette tanks. The rotating platter is mounted by its spindle on a wooden support and is turned by a motor, while the inner cylinder is held fixed at its top spindle. In use, the water level never exceeds the top of the inner cylinder.

Table 3. Organisms and stock culture methods. ATCC—American Type Culture Collection. Media: PS—Puget Sound seawater; YE—0.01% yeast extract; CM—ciliate medium (see text); WG—wheat grain. Food: RBA—resident bacterial assemblage (grown in situ); MA—mixed algae (*Isochrysis galbana, Micromonas pusilla,* and *Chroomonas selina*).

Protozoan species	Source	Size (μm)	Medium	Food	Temp. (°C)	Feeding behavior reference
BB3 (chrysomonad flagellate)	Puget Sound	4	PS + YE	RBA	13	
PS6 (chrysomonad flagellate)	Puget Sound	3	PS + YE	RBA	13	
Paraphysomonas sp. (chrysomonad flagellate)	D. Caron	4	PS + YE	RBA	13	Fenchel 1982*a*
Monosiga sp. (aloricate choanoflagellate)	ATCC No. 50154	3	PS + YE	RBA	18	Fenchel 1982*a*
Diaphanoeca grandis (loricate choanoflagellate)	ATCC No. 50111	5 (cell body) 20 (lorica)	CM + YE + f/2 Na_2SiO_3	RBA	8	Andersen 1988
Ciliophrys marina (helioflagellate)	T. Fenchel	10–15 (cell body) 30–100 (total)	PS @ 17‰ + WG	RBA	13	Davidson 1982
SmCil (heterotrich ciliate)	Chesapeake Bay	15	PS @ 20‰ + YE	RBA	18	
Helicostomella sp. (tintinnid ciliate)	Puget Sound	100–120 × 25 (lorica)	CM	MA	13	
Favella sp. (tintinnid ciliate)	Puget Sound	150–200 × 100 (lorica)	CM	MA*	13	Taniguchi and Takeda 1988

* *Gymnodinium simplex* added to MA.

Shimeta et al.

Table 4. Concentrations of protozoa and food particles in shear experiments.

Protozoan species	Protozoan concn (ml^{-1})*	Total food concn (ml^{-1})	Fluorescent food (%)
		Mean $\pm$ SE	
BB3[†]	1.2×10^3	$(1.9 \pm 0.2) \times 10^6$	46 ± 4
BB3[‡]	1.1×10^3	$(1.5 \pm 0.05) \times 10^6$	38 ± 2
PS6	3.0×10^3	$(1.4 \pm 0.1) \times 10^6$	76 ± 4
Paraphysomonas sp.	2.0×10^3	$(2.0 \pm 0.1) \times 10^6$	50 ± 1
Monosiga sp.[§]	7.4×10^3	$(1.5 \pm 0.1) \times 10^6$	71 ± 1
Monosiga sp.[‖]	9.6×10^3	$(2.6 \pm 0.04) \times 10^6$	35 ± 1
Diaphanoeca grandis	4.2×10^2	$(1.1 \pm 0.02) \times 10^6$	42 ± 1
Ciliophrys marina	4.1×10^2	$(4.5 \pm 0.4) \times 10^6$	42 ± 1
SmCil	7.5×10^1	4.9×10^6	23 ± 1
Helicostomella sp.	6.0×10^1	$(5.7 \pm 0.1) \times 10^3$	88 ± 0.2
Favella sp.	4.2×10^0	$(4.1 \pm 0.03) \times 10^3$	79 ± 0.1

* Calculated from the measured concentration in the inoculum.
[†] Experiment of clearance rate vs. shear rate in Fig. 4a.
[‡] Experiment of four repeated clearance-rate measurements at 1 s^{-1} in Fig. 4a.
[§] Experiment in Fig. 4e.
[‖] Experiment in Fig. 4f.

E. coli Genetic Stock Center (Yale University). Methods of culturing and harvesting minicells by sucrose density-gradient centrifugation followed those of Pace et al. (1990). Because *Ciliophrys* failed to ingest FLm at reasonably detectable rates, FLB were prepared from the bacteria in its stock culture (predominantly 2-μm long, nonmotile rods). Bacteria were grown overnight in 17‰ seawater with 0.01% yeast extract, having been inoculated with several milliliters of a *Ciliophrys* culture passed through a 1-μm syringe filter. Fluorescently labeled *Isochrysis galbana* ($\sim$5-μm diam) was prepared and used with *Helicostomella,* while fluorescently labeled *Gymnodinium simplex* ($\sim$10-μm diam) was used with *Favella.*

Growth cultures prior to experiments—Prior to feeding-rate measurements, a culture of protozoa (except for *Ciliophrys, see below*) was grown on unstained, live food cells of the type used for FLm or FLA. This culture step (the growth culture) presumably allowed protozoa to acclimate to feeding primarily on this food type. By the time protozoa were transferred to flasks or Couette tanks for feeding-rate measurements, residual cells of other food species from stock cultures were present at negligible concentrations. Growth cultures of bacterivores were in 100 ml of culture medium (no yeast extract), with an initial concentration of live unstained minicells of $\sim 10^7$ ml^{-1}. As a food source, live minicells served as an adequate substitute for marine bacteria, as evinced by a typical specific growth rate for *Monosiga* of 1.6 h^{-1} (data not shown), essentially identical to that measured by Fenchel (1982b) for this genus feeding on a marine *Pseudomonas.* Growth cultures of herbivores were in 1 liter of culture medium and were fed repeatedly over a week with only live *I. galbana* (for *Helicostomella*) or live *G. simplex* (for *Favella*). We took *Ciliophrys* directly from stock cultures for experiments because FLB were prepared from stock cultures. All cultures were harvested for experiments in late exponential growth.

Functional response—Feeding rates of each protozoan species were first measured in flasks of still water to determine the functional response (i.e. ingestion rate as a function of food concentration). Because the goal was merely to identify a nonsaturating food concentration for use in the shear experiment, as few as three treatments were run. All treatments for each species were run simultaneously with protozoa from a single growth culture (or stock culture, for *Ciliophrys*). Aliquots of culture were added to treatment flasks with fresh medium ($\sim$100 ml of total volume) and unlabeled food, as appropriate, and allowed to recover from handling for 30 min. For all bacterivores except *Ciliophrys* and *Diaphanoeca,* heat-killed unstained minicells were added as unlabeled food; live minicells were added as unlabeled food for *Diaphanoeca*; and for *Ciliophrys* and the herbivores, live food transferred from the stock culture and the growth cultures, respectively, served as unlabeled food. FLm, FLB, or FLA in 10 ml of culture medium were gently added to a flask, the flask was swirled, and a sample was taken to mark time zero. The percentages of total food cells that were labeled were similar to those used in shear experiments (Table 4). Four to six samples were taken at regular intervals over the course of 20–60 min, depending on the protozoan species. Samples of bacterivores were added directly to 10% NiSO$_4$ (0.5% final) to suppress egestion of food vacuole contents. All samples were fixed immediately with cold 10% glutaraldehyde (1% final).

Clearance rate as a function of shear rate—For each species, all treatments were run on one day with cells from a single growth culture (or stock culture, for *Ciliophrys*) and contained consistent concentrations of protozoa, total food, and percentage of labeled food in 100–150-ml total volume (Table 4). Labeled and unlabeled food were the same as in functional response experiments. Concentrations well below feeding saturation were chosen based on the functional response curves. Experiments
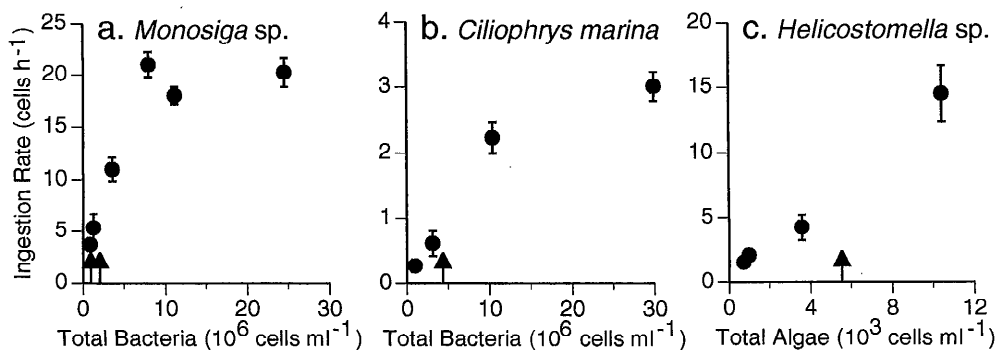
Fig. 3. Example functional response curves in still water (data for other species not shown). Points and error bars are the slopes and standard errors from linear regression of fluorescent-prey uptake over time. Arrows show concentrations used in subsequent shear experiments.

with BB3 and PS6 were run in only one Couette tank. Treatments were run in randomized order, and replication within a single day was not possible. A second experiment with BB3 was run to determine the variability of feeding rate at a single shear rate measured repeatedly in succession. Experiments with all other species were run in three simultaneously operating Couette tanks. Treatments and replicates were run in randomized order, with replicates of a single treatment run in different tanks. Each tank was run for 30 min to allow protozoa to acclimate before labeled food was added. The tank was turned off briefly while the inner cylinder was removed and labeled food was added in 10 ml of culture medium and gently stirred with a glass rod. The sample at time zero was taken after the tank was reassembled and turned on. Still-water treatments were run in the tanks with the motor off during acclimation and the experiment. We used polyethylene tubing (0.14-cm i.d.) attached to a syringe and inserted through a hole in the tank cover to gently withdraw samples from the side gap of the tank as it turned. Samples were taken at fixed intervals, preserved, and stored as described for functional response experiments.

Sample analyses—Samples were filtered onto Nuclepore black polycarbonate filters and examined with a Zeiss standard epifluorescence microscope. Pore sizes were 0.2 μm for counting bacteria, 0.8 μm for counting algae and examining small flagellates, and 1 or 2 μm for examining larger protozoa. Total bacterial and algal concentrations were counted from samples stained with acridine orange (Hobbie et al. 1977) from one or two time points and examined under blue light (Zeiss BP 450-490 excitation filter). Counts of FLm, FLB, and FLA were made similarly, but without staining. Samples for examining protozoa were stained with DAPI (Porter and Feig 1980) to identify cells by their nucleus under UV light (Zeiss G 365 excitation filter), and the numbers of ingested fluorescent food particles were counted by viewing under blue excitation. Between ~50 and 150 protozoa were examined in each sample. Samples from typically four or five time points (including time zero) from each replicate of each treatment were examined for ingested food particles.

For functional response data, the average number of ingested fluorescent food particles per protozoan cell at each time point was converted to the average total ingested food particles by multiplying by the ratio of total food to labeled food. Linear regression of the average total food particles ingested per cell against time was then performed. The slope was used as the measure of ingestion rate and its standard error as the measure of uncertainty. For Couette-tank experiments, the average number of ingested fluorescent food particles per protozoan cell at each time point was converted to the average clearance by dividing by the concentration of labeled food. Linear regression of the average clearance per cell against time yielded the clearance rate and its standard error. All linear regressions and nonlinear curve fits were performed with SYSTAT 5.2.1 software.

Results

Functional responses—Changes in feeding rates with food concentration (examples in Fig. 3) resemble standard functional responses for protozoa (e.g. Rivier et al. 1985). Ingestion rates rose approximately linearly at low food concentrations and leveled off at higher concentrations, where food availability saturates feeding capacity. Most of the curves revealed only a range of response in non-saturating conditions, but saturation was clearly reached with (e.g.) *Monosiga* at a bacterial concentration of 8×10^6 ml^{-1} (Fig. 3a). Also shown in Fig. 3 are the nonsaturating concentrations chosen for the corresponding Couette-tank experiments. If shear were to affect encounter rates with food particles (analogous to changing food concentrations), altered ingestion rates (higher or lower) could result and be measured.

Clearance rates as functions of shear rates—Four of the flagellates showed no significant effect of shear rate on clearance rate. For the chrysomonad BB3 (Fig. 4a), the variance of clearance rates measured repeatedly at 1.0 s^{-1} (points) was compared by an F-test (Sokal and Rohlf 1981) with the variance of clearance rates across shear rates (bars), yielding no significant difference ($P \approx 0.5$). Despite there being no a priori reason to expect a mono-
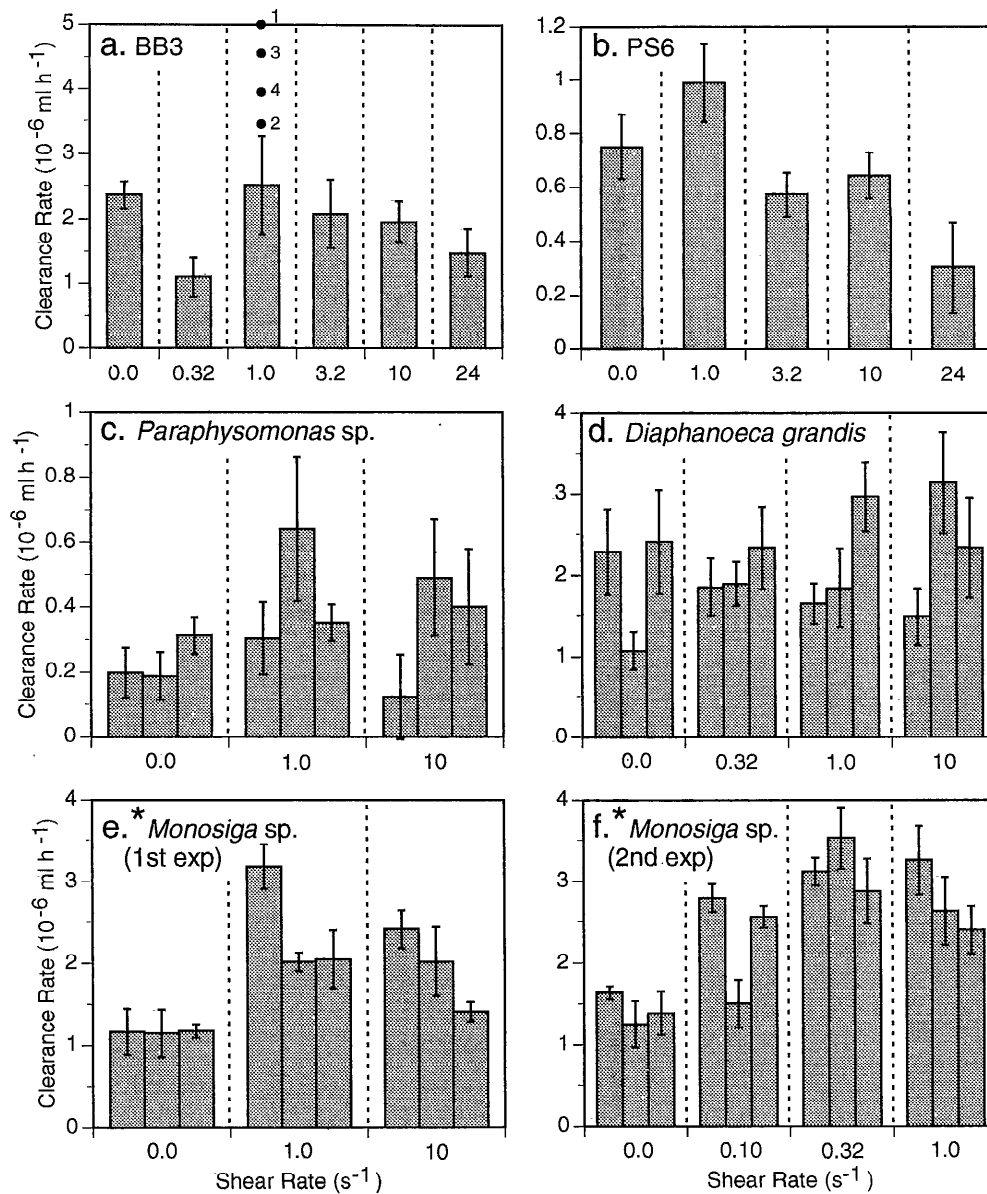
Fig. 4. Clearance rates in Couette tanks shown against categories of shear rate. *—Statistical significance at $\alpha = 0.05$. Each bar is a single measure, with height and error bar being the slope and standard error from linear regression of fluorescent-prey uptake over time. [a.] BB3 (linear regression through bars, not shown: slope $= -2.1 \pm 2.7 \times 10^{-8}$, $r^2 = 0.14$, $P = 0.47$). Points show repeated measures made separately at 1 s^{-1} (error bars omitted for clarity), with numbers indicating the order of execution. [b.] PS6 (linear regression slope $= -2.1 \pm 0.8 \times 10^{-8}$, $r^2 = 0.7$, $P = 0.075$). [c.] *Paraphysomonas* sp. (Kruskal-Wallis $P = 0.44$). [d.] *Diaphanoeca grandis* (K-W $P = 0.96$). [e.] *Monosiga* sp., 1st experiment (K-W $P = 0.025$). [f.] *Monosiga* sp., 2nd experiment (K-W $P = 0.018$). [g.] *Ciliophrys marina* (K-W $P = 0.00026$). [h.] *Helicostomella* sp. (K-W $P = 0.025$). [i.] *Favella* sp. (K-W $P = 0.83$). [j.] SmCil (K-W $P = 0.93$).

tonic trend, linear regression of clearance rate vs. shear rate (bars) was performed and yielded a nonsignificant slope ($P = 0.47$). The order in which runs were repeated at 1.0 s^{-1} showed no apparent relation to the measured clearance rates (Fig. 4a), suggesting that the feeding state of this flagellate did not change appreciably over the course of four runs. For the chrysomonad PS6 (Fig. 4b), linear regression yielded a nonsignificant slope ($P = 0.075$), and the variance of the clearance rates is not significantly

different from the variance of BB3's repeated measurements at 1.0 s^{-1} ($0.05 < P < 0.1$). For the chrysomonad *Paraphysomonas* (Fig. 4c), comparison of the three treatments with a Kruskal-Wallis (K-W) test indicated no significant difference ($P = 0.44$). The loricate choanoflagellate *Diaphanoeca grandis* also showed no significant effect (Fig. 4d, K-W $P = 0.96$).

In the first experiment with the aloricate choanoflagellate *Monosiga* (Fig. 4e), nonzero shear rates resulted
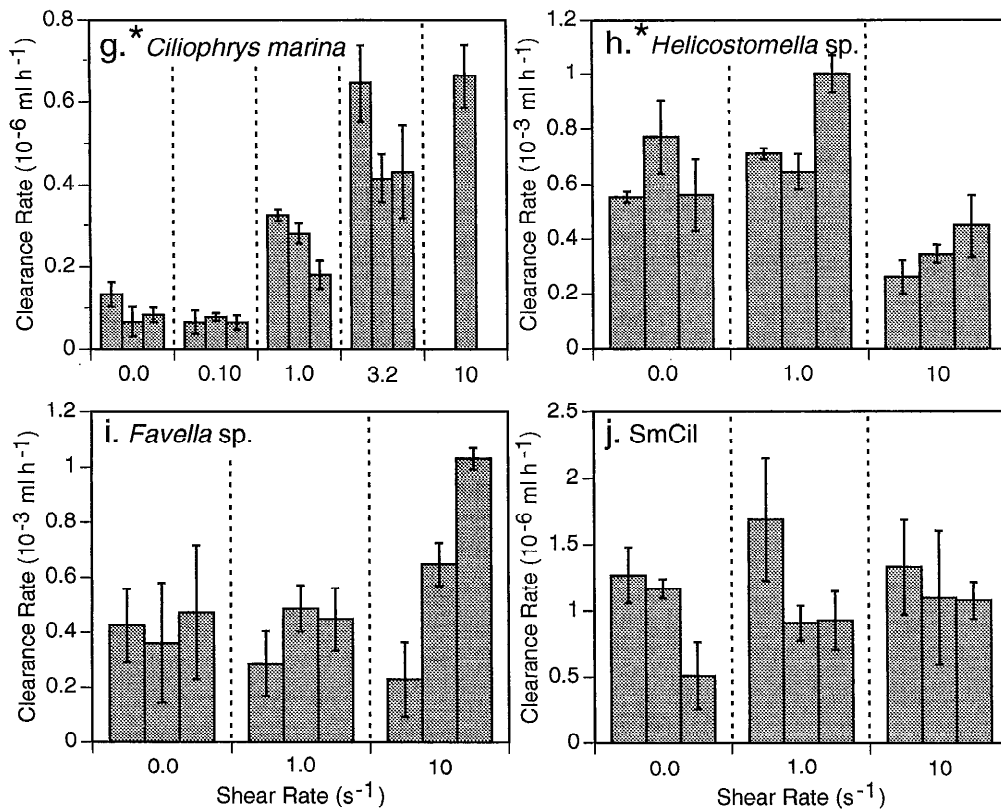
Fig. 4. Continued.

in elevated clearance rates over those in still water (K-W test for difference among treatments, $P = 0.025$). Multiple comparisons among treatments (Hollander and Wolfe 1973) revealed the greatest difference between 0 and 1.0 s^{-1} ($P = 0.029$), although the Bonferroni-corrected significance level is $\alpha = 0.016$ (Rice 1989). At 1.0 s^{-1}, the mean and the maximal clearance rates were 2.1× and 2.7× the mean in still water. A second experiment was run (Fig. 4f) in an attempt to replicate the first finding and achieve more resolution at lower shear rates, yielding a strongly significant result (K-W $P = 0.018$). Multiple comparisons revealed the greatest difference between 0 and 0.32 s^{-1} ($P = 0.012$), with a Bonferroni-corrected $\alpha = 0.008$. At 0.32 s^{-1}, the mean and the maximal clearance rates were 2.2× and 2.5× the mean in still water. Both experiments with *Monosiga* (Fig. 4e,f) suggest a saturation of clearance rate at high shear rates, which is particularly apparent when data from the second experiment are plotted on a continuous abscissa (Fig. 5a). At 0.1 s^{-1}, there is a trend of elevated clearance rates over still-water values, and we infer the threshold for an effect to be <0.1 s^{-1}. A sigmoid curve fits the data with $r^2 = 0.61$ (Fig. 5a), although there are no data at low nonzero shear rates that would clearly lie on the initially flat portion of the curve. Equivalent dissipation rates for measured effects and inferred thresholds are shown in Table 5.

The helioflagellate *Ciliophrys* (Fig. 4g) showed a sharp increase in clearance rate with shear rate, yielding a strongly significant difference among the four replicated treatments (K-W $P = 0.00026$). The greatest comparisonwise difference was between 0.1 and 3.2 s^{-1} ($P < 0.012$, Bonferroni-corrected $\alpha = 0.008$). At 3.2 s^{-1}, the mean and maximal clearance rates were 5.2× and 6.8× the still-water mean. The clearance rate at 10 s^{-1} was 7.0× the still-water mean. A sigmoid curve fits the data, with $r^2 = 0.91$ (Fig. 5b). Data at 0.1 s^{-1} lie on the initially flat part of the sigmoid (more easily seen on Fig. 4g); based on the trend of elevated clearance rates at 1 s^{-1}, we interpret the threshold for an effect to be between 0.1 and 1 s^{-1} (Table 5).

The tintinnid ciliate *Helicostomella* (Fig. 4h) showed a drop in clearance rates at 10 s^{-1}, with a significant difference among treatments (K-W $P = 0.025$). Multiple comparisons testing gave $P = 0.029$ (Bonferroni-corrected $\alpha = 0.016$) between 1.0 and 10 s^{-1}. At 10 s^{-1}, the mean and the minimal clearance rates were 0.56× and 0.42× the still-water mean.

No significant effects of shear were found for the other two ciliates: the tintinnid *Favella* (Fig. 4i, K-W $P = 0.83$) and the heterotrich SmCil (Fig. 4j, K-W $P = 0.93$).

Discussion

Couette-tank flow and particle dynamics—Rotating Couette flow has been well described and modeled (*see* van Duuren 1968). The shear in our tanks is steady, laminar, and approximately linear (≤6% deviation from the
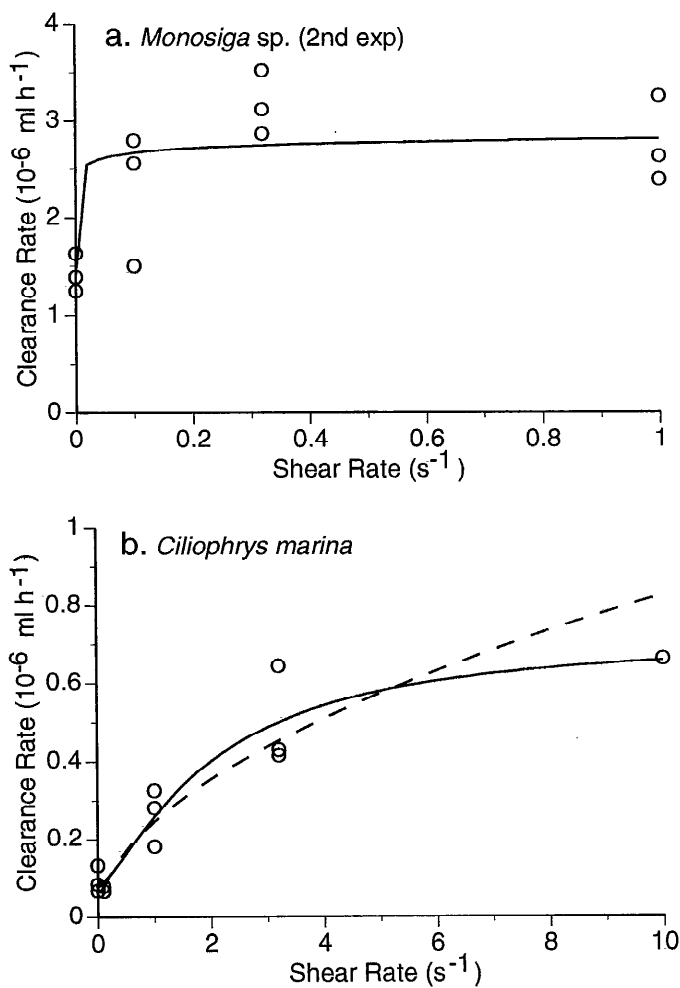
Shimeta et al.

Fig. 5. Clearance rates in Couette tanks plotted against shear rate. Error bars are omitted for clarity. [a.] *Monosiga* sp., 2nd experiment (Fig. 4f). The sigmoid curve is clearance = 1.78×10^{-6}shear$^{0.20}$/($0.26+$shear$^{0.20}$) + 1.40×10^{-6}; $r^2 = 0.61$. [b.] *Ciliophrys marina* (Fig. 4g). The sigmoid curve (solid) is clearance = 6.42×10^{-7}shear$^{1.38}$/($2.59+$shear$^{1.38}$) + 7.88×10^{-8}; $r^2 = 0.91$. The exponential curve (dashed), fitted to log-transformed data for 0.1–10 s^{-1}, is clearance = 2.45×10^{-7}shear$^{0.53}$; $r^2 = 0.94$; 95% C.I. on the exponent = 0.43–0.63.

mean), so there are essentially no microenvironments of exceptional flow conditions in which organisms could feed. The ratio of tank gap width to protozoan diameter ranged from 15 (*Favella*) to 1,000 (*Monosiga*), giving cells freedom to move without interference from the walls. Lift forces produced in shear flows cause particles to migrate across streamlines, e.g. toward the centerline of Couette flow (Leal 1980), but any concentrating effects on particle distributions should have been negligible in our experiments. Nonmotile food particles or *Ciliophrys* would have required ≥order 10^2 min to become concentrated in the center of the flow space, and motile cells should have had a ratio of swimming speed to lateral migration velocity of ≥order 10^1, allowing them to swim against lift forces (calculated for spheres according to Karp-Boss et al. in prep.).

Flows in the tanks differ from environmental, submicroscale shear in two important respects. First, the shear in a rotating Couette tank with large radius:gap ratio is essentially 1-dimensional, with a velocity gradient along a single axis (radial) normal to the flow, whereas submicroscale shear in the field is 3-dimensional. In Couette flow ("simple" shear flow), spherical particles rotate constantly, establishing a circulation region of "closed" streamlines that excludes approaching spheres on "open" streamlines from making contact (van de Ven 1982; Schowalter 1984). Upon close approach, however, two spheres can get caught in orbit around one another, and Brownian diffusion and van der Waals attraction have been invoked to explain final contact during particle coagulation. Analogous to Eq. 3, encounter rate by direct interception in Couette flow is modeled as

$$F_1 = \frac{4}{3}(r_1 + r_2)^3 G_C E_C C_2 \qquad (8)$$

where E_C is the collision efficiency in Couette flow (van de Ven 1982). The complex particle trajectories, incorporated into E_C, generally serve to reduce F_1 and result in F_1 scaling with G_C to a power less than unity.

Adler (1981) solved E_C numerically as a function of r_1, p ($=r_2/r_1$), G_C, and A, the Hamaker constant for van der Waals attraction. His model gives predictions of encounter rates that allow a comparison with our results to judge whether protozoa and bacteria behave like spheres in Couette flow. For the r_1 and G_C values from our *Ciliophrys* experiment (and assuming $A = 3.7 \times 10^{-21}$ J; Monger and Landry 1990), Adler's (1981) results show $F_1 \propto G_C^{0.16}$ when $p = 0.1$. Following the trend in Adler's results, the predicted proportionality would be even weaker for our $p \approx 0.02$. The exponential curve fitted to our data in Fig. 5b (dashed line), however, yields clearance rate $\propto G_C^{0.53}$

Table 5. Equivalent dissipation rates for measured effects of shear on feeding. Listed are only those species for which the data showed a statistically significant difference among shear-rate treatments. ε values were calculated with Eq. 2, assuming $G_C = G_t$. ε_{cons} values were calculated with Eq. 9. CR/CR$_0$ is the maximal measured clearance rate divided by mean clearance rate in still water. Threshold values bracket statistically nonsignificant trends in the data.

Protozoan species	Maximal observed effect			Threshold for effect	
	ε (W kg^{-1})	ε_{cons} (W kg^{-1})	CR/CR$_0$	ε_{cr} (W kg^{-1})	$\varepsilon_{(cons)cr}$ (W kg^{-1})
Monosiga sp.	7.5×10^{-6}	7.5×10^{-5}	2.7	$<7.5 \times 10^{-8}$	$<7.5 \times 10^{-7}$
Ciliophrys marina	7.5×10^{-4}	7.5×10^{-3}	7.0	7.5×10^{-8}–7.5×10^{-6}	7.5×10^{-7}–7.5×10^{-5}
Helicostomella sp.	7.5×10^{-4}	7.5×10^{-3}	0.42	7.5×10^{-6}–7.5×10^{-4}	7.5×10^{-5}–7.5×10^{-3}

(95% C.I. 0.43–0.63 for the exponent). Therefore, we observed a significantly stronger influence of shear rate on feeding rate than occurs for encounter between smooth spheres in Couette flow. The data for *Monosiga* (Fig. 5a) give insufficient information on the shape of the function because only two treatments revealed a response to an increase in nonzero shear rate (0.1 and 0.32 s^{-1}; note that 0 s^{-1} is still water and that feeding was clearly saturated between 0.32 and 1 s^{-1}). However, the magnitudes of clearance rates at all nonzero shear rates were 2–100× the predicted encounter rates from Adler (1981). Encounter rates matching these clearance rates would be predicted for shear much stronger than we used, meaning that we observed an effect of shear at a lower threshold shear rate than suggested by the model of spheres.

Several conclusions follow. First, models of sphere dynamics accounting for closed streamlines in Couette flow underpredict encounter rates between protozoa and their food particles, at least for *Ciliophrys* and *Monosiga* in our experiments. Encounter rates must equal or exceed measured ingestion rates, so the effects of shear on encounter rates were greater than they are for smooth spheres. It is likely that nonspherical morphologies (e.g. protruding pseudopodia) and feeding-swimming currents reduce or prevent an exclusion zone of closed streamlines around cells. However, for the more spherically shaped protozoa that showed no effect from shear (the chrysomonads), we cannot exclude the possibility that closed streamlines suppressed a response to rising shear rates. Our second conclusion, which follows from the first, is that models of spheres in turbulence (Eq. 3–5) may also apply poorly to protozoan feeding in the field. The qualitative prediction in Fig. 1 remains valid, but quantitative predictions of ε_{cr} from Eq. 4 and 5 (Tables 1, 2) are suspect. Equations 3–5 require a modified collision efficiency term specific to morphology and feeding mechanism. Our third conclusion is that if protozoan encounter rates are susceptible at all to artifacts of Couette-flow particle dynamics, our quantitative data may be conservative estimates of the influence of submicroscale shear in the field. A circulation region around a cell caused by flow-induced rotation may be less extensive and more ephemeral in turbulence than in Couette flow due to the 3-dimensional and time-varying nature of submicroscale shear. Such flow and cell motions are not well understood (Karp-Boss et al. in prep.), rendering the potential degree of conservativeness in our data uncertain.

The other important difference between flow in the Couette tanks and that below the turbulence microscale is that the Couette flow is steady, while environmental turbulence is highly intermittent. In the field, a period of a given shear rate at the microscale may last on the order of seconds to minutes, scaling as $(\nu/\varepsilon)^{1/2}$. Even for the highest ingestion rates measured here (order 10 cells h^{-1}) at typical field concentrations of food, a cell should go through most periods of relatively constant shear without ingesting any food. For this discussion, we assume that any observed effects of shear rate on clearance rate translate into differences in the probabilities of ingesting food among different periods of constant shear in the field.

Furthermore, in the absence of information on protozoan behavioral responses to time-varying flows, we assume that acclimation to changing shear strengths is instantaneous, such that the cumulative time that strong shear exists in the field can be considered without regard to its episodic pattern.

Dissipation rates in the surface mixed layer approximate a lognormal distribution, with a mode that typically can be an order of magnitude below the mean (Baker and Gibson 1987). When we equate G_C (Eq. 6, 7) with G_t (Eq. 2) to relate the steady shear rate in the Couette tank to a dissipation rate in the field, we obtain the equivalent of a "steady" dissipation rate that is stronger than the instantaneous turbulence experienced most of the time by organisms at such a mean dissipation rate. We can attempt to account roughly for this intermittency by converting G_C to an arbitrarily 10-fold higher, conservative dissipation rate:

$$\varepsilon_{cons} = 10(7.5\nu G_C^2) \qquad (9)$$

(compare with Eq. 2). At this mean dissipation rate, organisms in the field would experience instantaneous turbulence levels that are at least as strong as that corresponding to G_C for 90% of the time (according to the lognormal cumulative distribution function with variance parameter 1.5; Baker and Gibson 1987; Hastings and Peacock 1975).

Our conversions between the experimental G_C and a corresponding mean dissipation rate for the field (Table 5) are therefore rough for three reasons. First, Couette flow is qualitatively different from 3-dimensional environmental shear, yet we equate G_C with G_t. Second, there is disagreement in the literature regarding the proper coefficient to use in relating G_t to a directly corresponding mean dissipation rate, ε (Eq. 2); coefficients that have been used span a 6-fold range (*see introduction*). Third, our attempt to account for field intermittency of turbulence (ε_{cons}) is arbitrary but conservative.

Effects of shear on clearance rates—The measured effects of shear rate on feeding rates were species-specific. Three different responses were seen: no significant effect, enhancement of feeding rates at strong levels of shear, and suppression of feeding in extremely strong shear. Although measuring ingestion rates reveals the net effects of shear on feeding that are relevant to protozoan ecology, unequivocal interpretation of the results in terms of mechanisms of particle encounter, capture, and handling await direct visualization of both feeding-current flow fields and organism behavior under an imposed shear field. Where no effect of shear on feeding was observed, the possibility cannot be excluded that variations in encounter rates did occur but failed to be translated into altered ingestion rates. We offer hypotheses based on current understanding of functional morphologies to explain the results. It is encouraging that the species influenced by high shear rates are nonmotile or slow swimmers, consistent with a priori expectations (*see introduction*).

The three chrysomonad flagellates showed no significant effects of shear rate on clearance rates (Fig. 4a,b,c).

Paraphysomonas and the Puget Sound isolates, BB3 and PS6, were examined, respectively, up to shear rates corresponding directly to $\varepsilon = 7.5 \times 10^{-4}$ and 4.3×10^{-3} W kg^{-1}, or $\varepsilon_{cons} = 7.5 \times 10^{-3}$ and 4.3×10^{-2} W kg^{-1}, rates which are extremely rare in the environment. Peters and Gross (1994) also found no effect on ingestion rates for *Paraphysomonas imperforata* in a turbulence tank with a mean ε of order 10^{-3} W kg^{-1}, although cell division rates were elevated. Chrysomonads are roughly spherical (although *Paraphysomonas* is covered with scales) and can be very weak swimmers (e.g. 40 μm s^{-1} for *P. imperforata*; Eccleston-Parry and Leadbeater 1994), yet we suggest that it may be the very local details of the encounter mechanism that explain a lack of response to ambient shear. The chrysomonad feeding current pulls bacteria to the cell surface, where they directly intercept (Fenchel 1982a). Near the point of encounter, the separation distance between the centers of the flagellate and bacterium may be so small that the relative velocity created by the imposed shear is insignificant in comparison with the feeding-current flow field, which is highly nonuniform in that localized region. Note that the simple comparison between swimming speed and ambient shear in Eq. 4 assumes translation without a localized flow disturbance such as that created by a flagellum. The feeding mechanism, along with the small sizes of these cells (refer to the size dependence in Eq. 3 and 8), may therefore cause ε_{cr} to be beyond reasonable environmental levels. The consistency of results among the three taxa provides confidence in generalizing to chrysomonads and other nanoflagellates with similar morphology, such as bicoecids. We cannot exclude, however, that the impediment to contact between spheres in Couette flow is a significant effect for these roughly spherical protozoa.

The aloricate choanoflagellate *Monosiga* showed a strong response to shear (Figs. 4e,f and 5a). The maximal effect was measured in shear corresponding to very strong turbulence for the field, but the threshold dissipation rate for an effect may be in the range of moderate turbulence (Table 5). *Monosiga*'s feeding rate does not saturate until bacterial concentrations are $\geq 8 \times 10^6$ ml^{-1} (Fig. 3a), allowing for potentially similar influences of shear on feeding rates at field bacterial concentrations (e.g. 1×10^6 ml^{-1}).

We interpret elevated clearance rates under shear to result from enhanced encounter rates. Feeding in still water was encounter-rate limited because the food concentration was well below that for feeding-rate saturation. Elevated encounter rates caused by shear could therefore be analogous to raised levels of effective food concentration, and responses of higher feeding rates could ensue. It is not possible to exclude enhanced physical or behavioral means of retaining and ingesting bacteria once encountered, but it is counterintuitive that such responses would occur under stronger, as opposed to weaker, imposed flows. The growth culture allowed depletion of all bacteria other than minicells, so that experimental treatments contained essentially a single food type. Therefore, stained and unstained food was uniform in size and shape, eliminating the potential for differential encounter of stained cells based on their dynamics in shear flow.

In contrast to the chrysomonad feeding mechanism, choanoflagellates sieve particles through a collar of pseudopodia arising from the base of the beating flagellum (Fenchel 1986). The collar processes a much greater cross-sectional area of approaching fluid than does a chrysomonad, making the choanoflagellate's encounter mechanics potentially more susceptible to nonuniformity in ambient flow. Imposed shear may create sufficient relative motion between the choanoflagellate and a bacterium approaching near the distal portion of the collar to influence the encounter rate. Furthermore, *Monosiga* is known to be one of the slower swimming flagellates (30 μm s^{-1}; Fenchel 1982a), which is consistent with the prediction that weak swimmers are most susceptible to the influence of shear on feeding (*see introduction*). If the cell, including the tentacular collar, were a sphere of diameter 6 μm, Eq. 4 predicts that when swimming at 30 μm s^{-1} in turbulence, $\varepsilon_{cr} = 6 \times 10^{-5}$ W kg^{-1}. Our data in Couette flow, though, imply a threshold at least two orders of magnitude lower, and since the data disagree with Couette-flow predictions for spheres, the application of Eq. 4 is questionable.

If we assume a threshold shear rate does exist, the data in Fig. 5a are consistent with the shape of the hypothesized ingestion-rate curve in Fig. 1. Clearance rates leveled off at $G_C \geq 0.32$ s^{-1} (Figs. 4f, 5a), although the mechanism causing saturation must be different than that suggested in the introduction. *Monosiga*'s processing-limited ingestion rate is ~ 20 cells h^{-1} (Fig. 3a), well above the saturated rate of ~ 8 cells h^{-1} observed in the Couette tanks. The encounter rate should have continued to increase above a shear of 0.32 s^{-1}, and *Monosiga* should have been able to respond with a higher ingestion rate, so we suggest that the stronger shear field began to interfere with particle handling. Despite this possible interference, clearance rates were not strongly reduced at a shear of 10 s^{-1} (Fig. 4e), corresponding to $\varepsilon = 7.5 \times 10^{-4}$ W kg^{-1}, suggesting that very strong turbulence in the field would not significantly inhibit feeding.

The loricate choanoflagellate *Diaphanoeca grandis* showed no significant effect of shear rate on clearance rate up to 10 s^{-1} (Fig. 4d). Although *Diaphanoeca* is an extremely slow swimmer (5 μm s^{-1}), the lorica greatly constrains flow around the cell body (Andersen 1988). The lorica is partially covered by a membrane that exerts considerable drag on the swimming cell and channels flow past the tentacular collar. The lorica may therefore provide a refuge for the tentacular collar from ambient flow. We suggest that, in general, naked choanoflagellates are more susceptible to effects of turbulence than are loricate choanoflagellates.

The helioflagellate *Ciliophrys* showed a strong response to shear (Figs. 4g, 5b). The maximal effect was in shear corresponding to extremely strong turbulence for the field, but the threshold dissipation rate for an effect can be bracketed in the range of moderate turbulence (Table 5). *Ciliophrys*'s feeding rate at field concentrations of bacteria should be well below its maximal rate (Fig. 3b), allowing influence from turbulence in the field. We interpret the results with *Ciliophrys*, as for those with *Monosiga*, to be

caused by an effect of shear on encounter rates. *Ciliophrys* creates no feeding current (Davidson 1982), so relative motion from ambient flow must directly affect encounter rates, at least for nonmotile or weakly swimming prey.

The sigmoidal shape of the *Ciliophrys* data (Figs. 4g, 5b) agrees qualitatively with the shape of the ingestion-rate curve hypothesized in Fig. 1. The data at 0.1 s^{-1} are clearly below the threshold shear; however, Pe$_S$ ($=r_1^2 G_C/D$) predicts a much lower threshold of $\sim 4 \times 10^{-4}$ s^{-1} (assuming $r_1 = 30$ μm). It is possible that near 0.1 s^{-1} diffusional encounter dominated over direct interception (cf. model predictions of Shimeta 1993), resulting in an effect of shear that was too weak to observe. Models for spheres show that diffusional encounter rate is less strongly dependent on dissipation rate or shear rate than is direct interception rate. For example, in turbulence, diffusion rate $\propto \varepsilon^{1/6}$ (Shimeta 1993) and interception rate $\propto \varepsilon^{1/2}$ (Eq. 3); in simple shear, diffusion rate $\propto G_C^{0.5}$ and interception rate $\propto G_C^{0.8}$ (equal-sized spheres; van de Ven 1982). These patterns from sphere models may apply to protozoa even though the values of the exponents may not. The influence of shear may have approached saturation, as suggested by the single datum at 10 s^{-1} (Fig. 5b). This plateau might be due to a processing-rate limitation, as hypothesized in Fig. 1. The clearance rate there corresponds to an ingestion rate of 3 cells h^{-1}, near the saturation suggested in the functional response curve (Fig. 3b).

Ciliophrys was used here to represent the planktonic sarcodines, e.g. Radiolaria, Heliozoa, and Foraminifera (Davidson 1982; Caron and Swanberg 1990). Ambient flow may be most influential for these nonswimming taxa. Fenchel (1987) suggested that nonmotility renders the sarcodines diffusion feeders, relying on the motions of prey to cause encounter. Our experiments showed, however, that clearance rates on nonmotile bacteria are very strongly controlled by ambient shear rate in an environmentally relevant range. The radially symmetric morphology of sarcodines is consistent with a shear-encounter mechanism because environmental shear changes direction randomly and rotates the cells. Sarcodines eat algae and microzooplankton as well (Caron and Swanberg 1990). The nonmotile prey will be encountered by interception from the shear flow at higher particle-specific rates than bacteria because of their larger sizes. Based on Pe$_S$, we suggested in the introduction that turbulence might influence encounter of motile bacteria and motile phytoplankton (Table 2), although a predominance of diffusional encounter over direct interception in some range of ε could result in a weaker effect of shear. The calculation for encounter of ciliates by sarcodines suggested strongly that ε_{cr} is above the range of environmental turbulence (Table 2). We caution, though, that the swimming of many microplankters involves complex behaviors and discontinuous motions, such as jumping (Buskey et al. 1993), which render diffusion models inapplicable to small-scale movement patterns. These movements may make prey less likely to be advected by ambient shear, yet swimming behavior itself may be modified by turbulence (e.g. Hwang et al. 1994).

The only ciliate that showed a significant effect was *Helicostomella* (Fig. 4h), which had reduced clearance rates at shear corresponding to extremely strong turbulence (Table 5). *Helicostomella* is the slowest swimmer of the three ciliates, which might make it susceptible to disruption of its feeding current or particle-handling abilities under strong shear. We cannot, however, exclude the possibility of a behavioral response to strong shear (e.g. retraction into the lorica), which may or may not occur under environmental turbulence. *Favella*'s swimming velocity is among the highest of ciliates ($\sim 1,000$ μm s^{-1}; Buskey and Stoecker 1988), and there was no significant influence of shear for this species. Some ciliate populations can maintain aggregated distributions in the field despite turbulent diffusion (Jonsson 1989), suggesting that their swimming (and feeding) currents can dominate over ambient shear. Additional experiments with fast-swimming protozoans are required, however, to support the proposed mechanism that high swimming speeds prevent effects of realistic shear rates on feeding and to identify whether uncommonly high values of ε_{cr} do exist for such protozoans.

Ecological implications — Our results suggest that influences of turbulence on protozoan suspension feeding are species-specific. The majority of taxa we examined showed no response to an environmentally realistic range of shear rates. We hypothesize that the most significant effects of strong turbulence on feeding among the taxa studied take the form of enhanced rates for sarcodines (nonswimmers) and slow-swimming flagellates, particularly those that sieve particles. These groups include Radiolaria, Foraminifera, Heliozoa, helioflagellates, and choanoflagellates (although perhaps not the loricate or membrane-covered choanoflagellates). Exceptions to these generalizations are possible due to species-specific differences in functional morphology. The most intuitively appealing generalization to draw from this study is that nonswimming protists are the most affected by ambient water motion. Sarcodines can be numerically and ecologically important members of planktonic communities, although the distributions and ecological roles of actinopods are not as well known as for other protozoa (Caron and Swanberg 1990). Choanoflagellates are ubiquitous in marine environments, and in coastal and estuarine systems they can be ecologically important bacterivores, constituting as much as 50% by number of the heterotrophic flagellates (Fenchel 1986). Many choanoflagellates feed attached to surfaces, such as detritus, as do some members of the helioflagellates that feed similarly with a collar of pseudopodia (Fenchel 1986). Attached cells should also be susceptible to enhanced encounter rates in strong shear, perhaps even more than free-swimming cells because the increased drag from the attached particle raises the relative velocity and shear past the cell.

Effects of strong turbulence on suspension feeding by certain protozoan taxa imply a direct influence of the physical environment on population and community dynamics. Higher feeding rates under strong turbulence may lead to higher growth rates of the affected protozoa and greater impacts on their prey populations (cf. Peters and

Gross 1994). Encounter rates of suspension-feeding zooplankton larger than the microscale are also elevated under strong turbulence (Rothschild and Osborn 1988), although responses of feeding rates and growth rates can be complex (Marrase et al. 1990; Davis et al. 1991). It may be that feeding rates of selected zooplankton are accelerated throughout several levels of the food web by turbulence. Furthermore, the experiments suggest that current methods of measuring protozoan feeding rates in still-water incubations underestimate grazing by certain taxa under strong turbulence in the field.

Environmental turbulence varies greatly in space and time. Wind-driven turbulence is strongest near the surface, but other mechanisms such as current shear, internal waves, and convection can produce deeper local dissipation-rate maxima as well, e.g. at the top of the thermocline (Yamazaki and Osborn 1988). Fine-scale vertical distributions of protozoan suspension feeders in relation to water-column structure are not well known. In oceans and large lakes, ciliates can show peaks in concentration near the surface, the pycnocline, or subsurface chlorophyll maxima, although patterns can be inconsistent and explanations are debatable (Taylor and Heynen 1987; Jonsson 1989; E.J.L. unpubl. data). Less is known of nanoflagellate distributions, but peaks are sometimes seen at or below the depth of maximal bacterial or photosynthetic picoplankton abundances (Pick and Hamilton 1994). At the centimeter scale, biological patchiness can be correlated with hydrographic and turbulence microstructure (Owen 1989; Cowles and Desiderio 1993). Dynamics of the microbial food web may therefore be affected by small-scale variations in the "encounter-rate field" that are driven not only by variable plankton concentrations but also, for selected taxa, by variable turbulence. Turbulence levels in the surface mixed layer vary temporally on scales from minutes to days, as well as on a diurnal cycle (Oakey and Elliot 1982; Brainerd and Gregg 1993). Short-term responses of the microbial food web to isolated high-wind or mixing events or to diurnal patterns of mixing might be mediated through taxon-specific effects of turbulence on feeding.

Implications for suspension-feeding mechanics—Influences of submicroscale shear on encounter and feeding rates have several implications for generalizations commonly made regarding suspension-feeding mechanics. Reynolds numbers (Re) for flow over the bodies and appendages of many suspension feeders are ≪1, resulting in a strictly laminar flow regime at this scale (Shimeta and Jumars 1991). Low body-Re flow fields vary, however, depending on the steadiness and uniformity of the approaching flow, and thus they do not necessarily provide a refuge from larger scale, inertial flow phenomena. In turbulence, information from inertial phenomena is transferred to the viscous environment of protozoan suspension feeders in the form of a laminar shear field that can significantly influence feeding rates.

It has been common to classify suspension feeders as either active (relying on a particle flux created by feeding currents) or passive (relying on the ambient particle flux).

This distinction has been increasingly recognized as artificial in light of studies showing conventional active suspension feeders benefiting from ambient flow (Shimeta and Jumars 1991). Our study provides another such example: the feeding rate of a swimming choanoflagellate is augmented by the flux from ambient shear.

It has also been generalized that in the absence of a feeding current, protozoa feed from effectively still water and are dependent on prey motion to cause encounter (Fenchel 1982a, 1987). Our study suggests that encounter rates for a nonmotile-feeding species, *Ciliophrys,* are strongly dependent on relative flow, which always exists in the turbulent environment.

References

ADLER, P. M. 1981. Heterocoagulation in shear flow. J. Colloid Interface Sci. **83:** 106–115.
ANDERSEN, P. 1988. Functional biology of the choanoflagellate *Diaphanoeca grandis* Ellis. Mar. Microb. Food Webs **3:** 35–50.
BAKER, M. A., AND C. H. GIBSON. 1987. Sampling turbulence in the stratified ocean: Statistical consequences of strong intermittency. J. Phys. Oceanogr. **17:** 1817–1836.
BATCHELOR, G. K. 1980. Mass transfer from small particles suspended in turbulent fluid. J. Fluid Mech. **98:** 609–623.
BERDALET, E. 1992. Effects of turbulence on the marine dinoflagellate *Gymnodinium nelsonii.* J. Phycol. **28:** 267–272.
BOWEN, J. D., K. D. STOLZENBACH, AND S. W. CHISHOLM. 1993. Simulating bacterial clustering around phytoplankton cells in a turbulent ocean. Limnol. Oceanogr. **38:** 36–51.
BRAINERD, K. E., AND M. C. GREGG. 1993. Diurnal restratification and turbulence in the oceanic surface mixed layer. 1. Observations. J. Geophys. Res. **98:** 22,645–22,656.
BUSKEY, E. J., C. COULTER, AND S. STROM. 1993. Locomotory patterns of microzooplankton: Potential effects on food selectivity of larval fish. Bull. Mar. Sci. **53:** 29–43.
——, AND D. K. STOECKER. 1988. Locomotory patterns of the planktonic ciliate *Favella* sp.: Adaptations for remaining within food patches. Bull. Mar. Sci. **43:** 783–796.
CARON, D. A., AND N. R. SWANBERG. 1990. The ecology of planktonic sarcodines. Rev. Aquat. Sci. **3:** 147–180.
COWLES, T. J., AND R. A. DESIDERIO. 1993. Resolution of biological microstructure through in situ fluorescence emission spectra. Oceanography **6:** 105–111.
DAVIDSON, L. A. 1982. Ultrastructure, behavior, and algal affinities of the helioflagellate *Ciliophrys marina,* and the classification of the helioflagellates (Protista, Actinopoda, Heliozoea). J. Protozool. **29:** 19–29.
DAVIS, C. S., G. R. FLIERL, P. H. WIEBE, AND P. J. S. FRANKS. 1991. Micropatchiness, turbulence and recruitment in plankton. J. Mar. Res. **49:** 109–151.
ECCLESTON-PARRY, J. D., AND B. S. C. LEADBEATER. 1994. A comparison of the growth kinetics of six marine heterotrophic nanoflagellates fed with one bacterial species. Mar. Ecol. Prog. Ser. **105:** 167–177.
FENCHEL, T. 1980. Suspension feeding in ciliated protozoa: Structure and function of feeding organelles. Arch. Protistenk. **123:** 239–260.
——. 1982a,b. Ecology of heterotrophic microflagellates. 1. Some important forms and their functional morphology. 2. Bioenergetics and growth. Mar. Ecol. Prog. Ser. **8:** 211–223, 225–231.

——. 1986. The ecology of heterotrophic microflagellates. Adv. Microb. Ecol. **9:** 57–97.

——. 1987. Ecology of protozoa. Springer.

GARGETT, A. E. 1989. Ocean turbulence. Annu. Rev. Fluid Mech. **21:** 419–451.

GUILLARD, R. R. L. 1975. Culture of phytoplankton for feeding marine invertebrates, p. 29–60. *In* W. L. Smith and M. H. Chanley [eds.], Culture of marine invertebrate animals. Plenum.

HASTINGS, N. A. J., AND J. B. PEACOCK. 1975. Statistical distributions. Butterworth.

HELLUNG-LARSEN, P., AND I. LYHNE. 1992. Effect of shaking on the growth of diluted cultures of *Tetrahymena*. J. Protozool. **39:** 345–349.

HILL, P. S. 1992. Reconciling aggregation theory with observed vertical fluxes following phytoplankton blooms. J. Geophys. Res. **97:** 2295–2308.

HOBBIE, J. E., R. J. DALEY, AND S. JASPER. 1977. Use of Nuclepore filters for counting bacteria by fluorescence microscopy. Appl. Environ. Microbiol. **33:** 1225–1228.

HOLLANDER, M., AND D. A. WOLFE. 1973. Nonparametric statistical methods. Wiley.

HWANG, J.-S., J. H. COSTELLO, AND J. R. STRICKLER. 1994. Copepod grazing in turbulent flow: Elevated foraging behavior and habituation of escape responses. J. Plankton Res. **16:** 421–431.

JONSSON, P. R. 1989. Vertical distribution of planktonic ciliates—an experimental analysis of swimming behaviour. Mar. Ecol. Prog. Ser. **52:** 39–53.

LAZIER, J. R. N., AND K. H. MANN. 1989. Turbulence and the diffusive layers around small organisms. Deep-Sea Res. **36:** 1721–1733.

LEAL, L. G. 1980. Particle motions in a viscous fluid. J. Fluid Mech. **12:** 435–476.

MARRASE, C., J. H. COSTELLO, T. GRANATA, AND J. R. STRICKLER. 1990. Grazing in a turbulent environment: Energy dissipation, encounter rates, and efficacy of feeding currents in *Centropages hamatus*. Proc. Natl. Acad. Sci. **87:** 1653–1657.

MONGER, B. C., AND M. R. LANDRY. 1990. Direct-interception feeding by marine zooflagellates: The importance of surface and hydrodynamic forces. Mar. Ecol. Prog. Ser. **65:** 123–140.

OAKEY, N. S., AND J. A. ELLIOT. 1982. Dissipation within the surface mixed layer. J. Phys. Oceanogr. **12:** 171–185.

OWEN, R. W. 1989. Microscale and finescale variations of small plankton in coastal and pelagic environments. J. Mar. Res. **47:** 197–240.

PACE, M. L., G. B. MCMANUS, AND S. E. G. FINDLAY. 1990. Planktonic community structure determines the fate of bacterial production in a temperate lake. Limnol. Oceanogr. **35:** 795–808.

PETERS, F., AND T. GROSS. 1994. Increased grazing rates of microplankton in response to small-scale turbulence. Mar. Ecol. Prog. Ser. **115:** 299–307.

PICK, F. R., AND P. B. HAMILTON. 1994. A comparison of seasonal and vertical patterns of phagotrophic flagellates in relation to bacteria and algal biomass in temperate lakes. Mar. Microb. Food Webs **8:** 201–215.

PORTER, K. G., AND Y. S. FEIG. 1980. The use of DAPI for identifying and counting aquatic microflora. Limnol. Oceanogr. **25:** 943–948.

REAL, L. A. 1977. The kinetics of functional response. Am. Nat. **111:** 289–300.

RICE, W. R. 1989. Analyzing tables of statistical tests. Evolution **43:** 223–225.

RIVIER, A., D. C. BROWNLEE, R. W. SHELDON, AND F. RASOULZADEGAN. 1985. Growth of microzooplankton: A comparative study of bacterivorous zooflagellates and ciliates. Mar. Microb. Food Webs **1:** 51–60.

ROBERTS, A. M. 1981. Hydrodynamics of protozoan swimming, p. 5–66. *In* M. Levandowsky and S. H. Hutner [eds.], Biochemistry and physiology of protozoa. V. 4. Academic.

ROTHSCHILD, B. J., AND T. R. OSBORN. 1988. Small-scale turbulence and plankton contact rates. J. Plankton Res. **10:** 465–474.

SAFFMAN, P. G., AND J. S. TURNER 1956. On the collision of drops in turbulent clouds. J. Fluid Mech. **1:** 16–30.

SCHOWALTER, W. R. 1984. Stability and coagulation of colloids in shear fields. Annu. Rev. Fluid Mech. **16:** 245–261.

SHERR, B. F., E. B. SHERR, AND C. PEDRÓS-ALIÓ. 1989. Simultaneous measurement of bacterioplankton production and protozoan bacterivory in estuarine water. Mar. Ecol. Prog. Ser. **54:** 209–219.

SHERR, E. B., AND B. F. SHERR. 1993. Protistan grazing rates via uptake of fluorescently labeled prey, p. 695–701. *In* P. F. Kemp et al. [eds.], Handbook of methods in aquatic microbial ecology. Lewis.

SHIMETA, J. 1993. Diffusional encounter of submicrometer particles and small cells by suspension feeders. Limnol. Oceanogr. **38:** 456–465.

——, AND P. A. JUMARS. 1991. Physical mechanisms and rates of particle capture by suspension-feeders. Oceanogr. Mar. Biol. Annu. Rev. **29:** 191–257.

SOKAL, R. R., AND F. J. ROHLF. 1981. Biometry. Freeman.

TANIGUCHI, A., AND Y. TAKEDA. 1988. Feeding rate and behavior of the tintinnid ciliate *Favella taraikaensis* observed with a high speed VTR system. Mar. Microb. Food Webs **3:** 21–34.

TAYLOR, W. D., AND M. L. HEYNEN. 1987. Seasonal and vertical distribution of Ciliophora in Lake Ontario. Can. J. Fish. Aquat. Sci. **44:** 2185–2191.

TENNEKES, H., AND J. L. LUMLEY. 1972. A first course in turbulence. MIT.

THOMAS, W. H., AND C. H. GIBSON. 1990. Quantified small-scale turbulence inhibits a red tide dinoflagellate, *Gonyaulax polyedra* Stein. Deep-Sea Res. **37:** 1583–1593.

VAN DE VEN, T. G. M. 1982. Interactions between colloidal particles in simple shear flow. Adv. Colloid Interface Sci. **17:** 105–127.

VAN DUUREN, F. A. 1968. Defined velocity gradient model flocculator. J. Sanit. Eng. Div. Proc. ASCE **94:** 671–682.

VAN WAZER, J. R., J. W. LYONS, K. Y. KIM, AND R. E. COLWELL. 1963. Viscosity and flow measurement. Interscience.

WESSON, J. C., AND M. C. GREGG. 1994. Mixing at Camarinal Sill in the Strait of Gibraltar. J. Geophys. Res. **99:** 9847–9878.

YAMAZAKI, H., AND T. R. OSBORN. 1988. Review of oceanic turbulence: Implications for biodynamics, p. 215–234. *In* B. J. Rothschild [ed.], Toward a theory on biological-physical interactions in the world ocean. Kluwer.